

## Charting the Course to Resilience: Hydrodynamic Modeling for Socio-economic Insights for Flood Risk Management in Nepal's Ungauged Roshi River Catchment

SUNIL DUWAL<sup>1,\*</sup>, YOGESH BHATTARAI<sup>1</sup>, RABINA MILAPATI<sup>2</sup>, AND ROCKY TALCHABHADEL<sup>3</sup>

<sup>1</sup>*Department of Civil Engineering, Khwopa College of Engineering, Bhaktapur, Nepal.*

<sup>2</sup>*Department of Environmental Science, Khwopa College, Bhaktapur, Nepal.*

<sup>3</sup>*Department of Civil and Environmental Engineering, Jackson State University, Mississippi, USA.*

(Received 03 August 2023; Accepted 06 October 2023)

### ABSTRACT

Nepal, a Himalayan country with diverse topography, faces significant flood risks yearly. This study focuses on flood hazard mapping and vulnerability assessments for the Roshi River catchment (RRC), situated in the mid-hills of Nepal, by using hydrodynamic modeling and scenario-based approaches. The results obtained from probability distribution methods revealed varying flood magnitudes from 100 m<sup>3</sup>/s to 1100 m<sup>3</sup>/s. Inundations analysis showed plains near the Araniko Highway (AH42) and Panauti Municipality to be high-risk flood-prone areas. Croplands are the most susceptible, while the estimated number of people and buildings at risk varies from 4,000 to 7000 people in 1200 to 2600 buildings. Socio-economic analysis shows that a major portion of the population is from Tamang ethnicity, with relatively lower economic and educational status. Similarly, women in economically and socially disadvantaged communities are particularly at risk, emphasizing the need for increased awareness and support. Proactive flood disaster management strategies are crucial, especially for marginalized and agriculture-dependent communities. The strategically important RRC's link to key cities, including Kathmandu, demands effective flood control measures. Hydrodynamic modeling with possible scenarios relating to socio-economic aspects can aid decision-making processes from local to central government levels to create a more resilient and disaster-resistant future for Nepal.

**Keywords:** Flood Hazard Mapping, Hydrodynamic Model, Scenario-based modeling, Roshi River Catchment.

### 1. Introduction

Floods are one of the disastrous natural hazards that wreak havoc on human lives and infrastructure (Zotou et al., 2022). These calamities occur when water surpasses the capacity of natural structures like rivers, lakes, and dams, inundating nearby floodplains (Merz et al., 2021; Namara et al., 2022). Due to population growth and economic development in flood-prone areas, flood exposure is projected to increase by 2050, leading to more casualties and damage (Afzal et al., 2022; Merz et al., 2021). Between 2000 and 2019, global flood damages reached a staggering \$651 billion (Tellman et al., 2021). Human activities, such as land use changes and climate shifts, significantly amplify flood hazards, posing severe threats to society, the environment, and the economy (Pinos and Timbe, 2019; Sofia and Nikolopoulos, 2020). With over 1 billion people residing in floodplains, measuring flood risk, exposure, and vulnerability becomes imperative for disaster mitigation (Yin et al., 2018).

Nepal, a developing nation, faces rapid population growth and heightened vulnerability to various disasters, including earthquakes, droughts, floods, landslides, extreme temperatures, and glacial lake outburst floods (GLOFs) that impact more than 80% of the population (UNDRR, 2019). Inadequate management of floodplains in Nepal has dire consequences, with floods alone causing 29% of annual deaths and 43% of total property losses (Aryal et al., 2020). Between 1971 and 2020, Nepal witnessed over 5,000 flood disasters, resulting in more than 4,000 fatalities (Sharma et al., 2023). In 2017, floods destroyed 41,625 houses, damaged 150,510 more, and incurred an economic loss of \$187.9 million (Thapa et al., 2020). Internal migration due to floods exceeded 99,000 people from 2008 to 2021, with 32,000 occurring in 2021 alone (Anzellini Vicente, 2022). The impact on agriculture and food security further compounds the plight of low-income, uneducated, and unemployed individuals forced to remain in flood-prone areas (Shreevastav et al., 2021). Vulnerability studies often overlook the multifaceted effects of disasters like floods (Guragain and Doneys, 2022). Farmers and disadvantaged groups in Nepal bear a disproportionate burden of flood-related hazards (Pathak et al., 2020). The country's economy is intricately linked to mon-

\*Corresponding author: Sunil Duwal, Department of Civil Engineering, Khwopa College of Engineering, Bhaktapur, Nepal. Email: duwal.sunil@khwopa.edu.np

soon rainfall patterns, which, if excessive, lead to catastrophic flooding (Jha et al., 2016; Pathak et al., 2020). Despite previous studies (Aryal et al., 2020; Dangol, 2014; Dangol and Bormudoi, 2015), Nepal's flood hazard management remains hindered by socio-economic limitations, insufficient monitoring data, and the disconnection between scientific knowledge and community understanding (Sharma et al., 2023). For effective flood hazard management, flood inundation mapping and potential damage estimate through a probabilistic approach are essential (Pinos and Timbe, 2019; Thapa et al., 2020). By harnessing increased capabilities of geoinformatics, Nepal can enhance long-term planning and flood control measures (Dangol, 2014). Annual monsoon floods from June to September continually afflict Nepal (Thapa et al., 2020). Climatic changes, shifts in rainfall patterns Talchabhadel et al. (2018), land use alterations (Lamichhane and Shakya, 2019), and the proliferation of crusher industries and their sediment deposits exacerbate flood risks (Talchabhadel et al., 2021). Flood hazard mapping is essential for reducing community impact since flood events are uncontrollable. Comprehensive planning and non-structural measures can help minimize damage (Thapa et al., 2020).

Advancements in computing power have made numerical flood simulations more accessible. Flood models now employ cutting-edge remote sensing and hydrodynamic modeling techniques to identify flood-prone areas (Hosseiny et al., 2020). However, a major challenge in flood estimation and risk assessment is the scarcity of long-term data spanning over a century. Researchers have explored various peak flood estimation methods, often relying on historical data and spatially similar regions (Halbert et al., 2016; Yue et al., 1999). Flood frequency analysis, combined with hydrodynamic modeling, minimizes uncertainty in river discharge predictions, preventing costly investments in floodplain management and protection structures (Bomers et al., 2019; Sarchani et al., 2020). Risk analyses increasingly emphasize accounting for uncertainties (Merz and Thielen, 2005). Scenario-based approaches provide a means to address uncertainties by introducing confidence intervals to quantify sampling errors in statistics (Chowdhury and Stedinger, 1991). In developing countries like Nepal, reliable hydrological data are scarce (Sharma et al., 2019), adding natural and epistemic uncertainties to hydrologic analysis (Merz and Thielen, 2005). These uncertainties significantly affect flood estimations, especially with the added uncertainty brought by climate change. For instance, the design flood could increase dramatically with climate change, as seen in a study on the Koshi River (Devkota and Gyawali, 2015), which projected the 100- and 500-year flood return periods to be equivalent to 1,000 and 10,000 years, respectively. We employed scenario-based flood estimations in our hydrodynamic modeling for flood inundation mapping to address these complexities. Mapping the spatial distribution of hydraulic charac-

teristics aids in creating flood inundation maps, offering insights into flow depths, patterns, and water movement toward floodplains (Hosseiny et al., 2020; Namara et al., 2022; Pinos and Timbe, 2019). Accurate representation of river geometry, including channels, banks, flow paths, and topography, is crucial for one-dimensional hydrodynamic modeling, focusing on horizontal river paths and flood areas (Afzal et al., 2022; Sarchani et al., 2020). The Hydrologic Engineering Center-River Analysis System (HEC-RAS), developed by the US Army Corps, serves as an invaluable tool for river system modeling, integrating geographic information (Afzal et al., 2022; Aryal et al., 2020; Zotou et al., 2022). Our study employed HEC-RAS to model the Roshi River in the mid-hills of Nepal originating from the foothills of Phulchowki, characterized by steep slopes and high erosive capacity downstream (Poudel et al., 2012). Population growth, sand extraction from riverbanks, development near the BP highway, and unauthorized waste disposal have increased flood hazards in the Roshi River (Singh, 2018). Sediment deposition reduces the river channel's capacity, leading to expanded inundation areas during flood events (Dingle et al., 2020). The climate variability observed throughout the country, including this area, exacerbates the region's flooding yearly.

Hazard studies are constrained by the uncertainty in hazard models brought on by difficulties combining rapid anthropogenic change, insufficient calibration data, and substandard topography data (Tellman et al., 2021). This scenario has motivated us to prepare the Roshi River Catchment (RRC) flood hazard mapping based on hydrodynamic modeling. Previous studies (Aryal et al., 2020) focused on the hydrodynamic modeling of the gauged river basin where data were available; however, our study employs hydrodynamic modeling to assess socio-economic impacts in Nepal's ungauged river basin. A flood vulnerability assessment is crucial for informed decision-making and proactive risk mitigation (Pathak et al., 2020). Using HEC-RAS, we modeled the Roshi River to identify flood-prone areas for return periods of 2, 5, 10, 25, 50, 100, 200, and 500 years to create scenario-based hazard maps, creating scenario-based hazard maps. This assessment aims to connect decision-making processes by considering population, buildings, land use, and socio-economic factors, ultimately aiding in developing adaptation strategies and strengthening community resilience.

## 2. Study Area and Data

### 2.1. Study Area

The Roshi River serves as one of the tributaries of the Sunkoshi River in the central-eastern portion of Nepal. It is spring-fed and converges on the Sunkoshi River near the small settlements of Dumja. Interviews with the locals revealed that the name of the river originated from the small

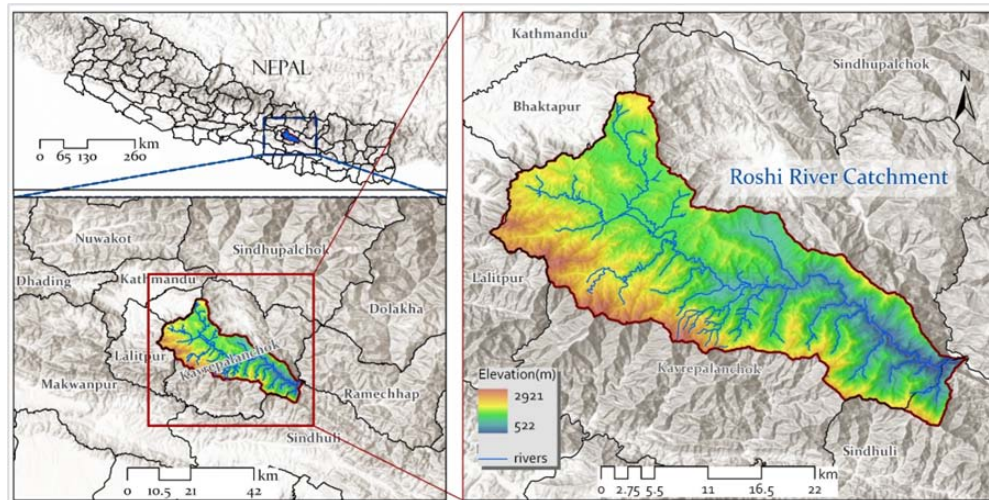


FIG. 1. Location map of the Roshi River Catchment.

village of Roshi Gaon, three kilometers from the old historic Newar town of Panauti. The catchment has an area of 565 km<sup>2</sup>. The study area emphasizes the section of the Punyamata River by the side of Araniko Highway (Area near the Banepa Municipality) upstream of the Panauti confluence of the Punyamata River to the convergences of the Roshi River to Sunkoshi. This section of Punyamata includes Banepa and Dhulikhel Municipalities, one of the fastest-growing municipalities. The Roshi River flows through Panauti Municipality, Roshi Rural Municipality, Namobuddha Municipality, Bethanchok Rural Municipality, Temal Rural Municipality, and Sunkoshi Rural Municipality. Forests account for most of the land use in the RRC (47.7%), followed by cultivated land (44.7%).

## 2.2. Data

We acquired hydrological data for the Sunkoshi River (ID = 652) from 1968 to 2015 and long-term average precipitation data for RRC from the Department of Hydrology and Meteorology (DHM), Nepal. We used a 30m x 30m digital elevation model (DEM) from the Advanced Spaceborne Thermal Emission and Reflection Radiometer (ASTER). To identify inundation areas, we used Sentinel-1 SAR satellite data from the Copernicus Open Access Hub of the European Space Agency (<https://scihub.copernicus.eu/>). Land use/land cover (LULC) information for 2019 came from the International Center for Integrated Mountain Development (ICIMOD). Data on buildings, settlements, bridges, hospitals, and schools were extracted from OpenStreetMap. We adjusted population data with a 1 ha. x 1 ha. spatial resolution using the United Nations Secretariat's Population Division data (<https://hub.worldpop.org/>). Data and statistics about the 2021 census were obtained from the National

Statistics Office (<https://censusnepal.cbs.gov.np>). Ground truth validation points were collected through field visits and local people's interviews.

## 2.3. Methodology

The study in RRC involves two main parts: a) Hydrological analysis, including estimating flood discharge and frequency analysis, and b) Hydrodynamic modeling using HEC-RAS to assess vulnerability to buildings, land use, and people (Figure 2). If the ungauged basins are hydrologically and physiologically similar and neighboring geographically, then the transfer of information, such as stream flows, seems suitable (Razavi and Coulibaly, 2013). The RRC is a part of the Sunkoshi River Basin, so the flow data from the closest hydrologic stations was used to transfer the flood data to the RRC. To transfer the extreme discharge data from the Sunkoshi River Basin catchment-area ratio (CAR) (Asquith et al., 2006; Emerson et al., 2005) was utilized. It involves multiplying the long-term data from a hydrologically similar catchment (HSC) by the ratio of the catchment areas of the proposed site (base station) and the HSC.

$$Q_b = Q_i \frac{A_b}{A_i} \quad (1)$$

where Q = discharge in m<sup>3</sup>/s, A = drainage area in km<sup>2</sup>, 'b' stands for base station, and i stands for index station. Besides physiological similarities in the catchments, the rainfalls, the most crucial factor for runoff generation, may vary. So, the flood data derived from the CAR method were re-adjusted using the precipitation ratio using precipitation data from the rain gauge stations in and around the catchment. The point rainfall data were spatially interpolated using three methods: a) Kriging, b) Inverse Distance Weightage (IDW), and c) Nearest Neighborhood

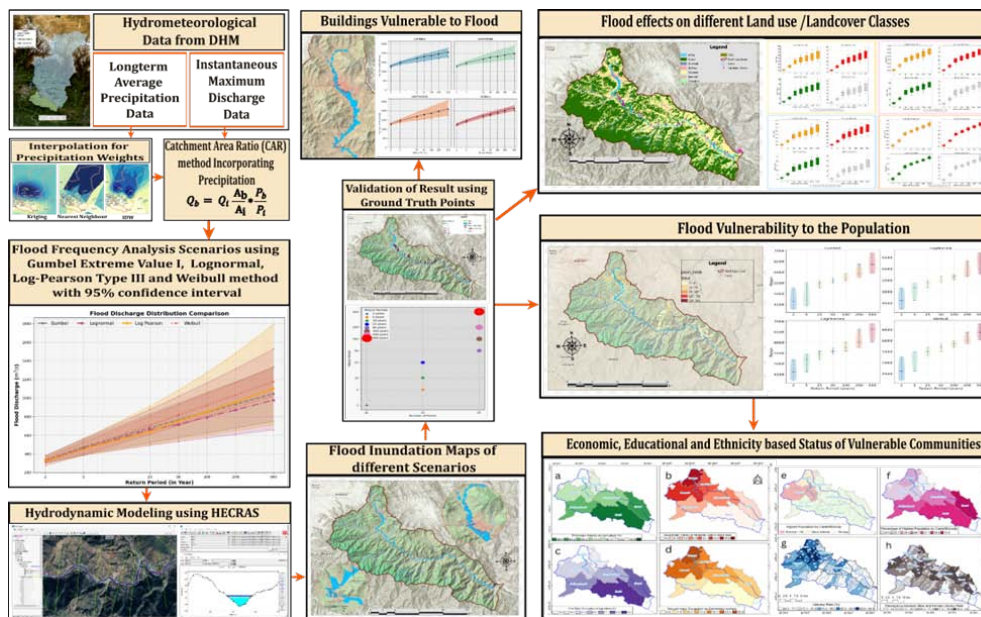


Fig. 2. Framework for identifying the prone area for flood risk reduction using a hydrodynamic model.

(NN) Method. We used the spatial average of the rainfall to calculate the weights for precipitation adjustment. Thus, the flood discharge for base station ‘b’ was adjusted as

$$Q_b = Q_i \frac{A_b}{A_i} \times \frac{P_b}{P_i} \quad (2)$$

$P_b$  and  $P_i$  are precipitation weights of base and index stations, respectively.

We performed the flood frequency analysis to determine the flood magnitudes for different return periods using Log Pearson Type III (LP-III), Log Normal (LN), Gumbel’s Extreme Value I (GEV-I), and Weibull’s (WB) methods. These are popular distributions used in flood analysis (Maposa et al., 2014). We performed a goodness of fit test using the Kolmogorov-Smirnov test (KS)(Maposa et al., 2014; Rahman et al., 2013) to test the applicability of the results from these distributions. For the estimation of floods for the corresponding return period, the Chow formula was used.

$$X_T = \bar{X} + K_T \sigma \quad (3)$$

where  $X_T$  is the estimated flood discharge for the Return period (T),  $\bar{X}$  is the mean of the yearly extreme discharge,  $K_T$  is the frequency factor, and  $\sigma$  is the standard deviation. A 95% confidence limit was used to evaluate the upper and lower limits.

This study adopted steady-flow hydrodynamics governed by the Continuity and Momentum equations. We started Hydrodynamic modeling in the HEC-RAS by developing the Roshi River’s geometry, which includes the

construction of the river’s centerline, left banks, right banks, and cross-sections. The selection of a suitable roughness coefficient is essential for the better performance of the hydrodynamic model (Tegos et al., 2022), so after constructing geometry, the values of Manning’s roughness coefficient ‘n’ were assigned based on the LULC classification map as recommended by (Chow, 1959), as shown in Table 1. We performed a 1D-steady flow run under mixed flow regime conditions using the discharge values obtained from an LN, LP-III, GEV-I, and WB method for different return periods with limits estimated from 95% confidence intervals to create water profiles in HEC-RAS. These profiles were then transferred to the QGIS interface for flood inundation mapping. Information about buildings, roads, hospitals, and other physical infrastructure in the RRC was extracted from OSM. We used Landsat8, Sentinel2, and MODIS imagery to delineate water bodies and compared with the result from HEC-RAS as done by (Afzal et al., 2022; Tamiru and Dinka, 2021; Zotou et al., 2020). In most cases, the Normalized Difference Water Index (NDWI) is utilized to reference the flood inundation area (McFeeters, 1996; Tamiru and Dinka, 2021), as shown in equation 3.

$$NDWI = \frac{GREEN - NIR}{GREEN + NIR} \quad (4)$$

$$MNDWI = \frac{GREEN - SWIR}{GREEN + SWIR} \quad (5)$$

However, as the flood water contains sediments in massive amounts, it would be better to use Modified NDWI (MNDWI) as in equation 7 to assess the flood area accurately. Likewise, high water level marks observed during

TABLE 1. Assigned Manning's Roughness Coefficients (n) to LULC classes.

class	Cropland	Built-up	Riverbed	Forest	Grassland	Other	Wooded Land (OWL)	Bare Soil	Unclassified
Manning's (n)	0.115	0.035	0.02	0.275	0.3		0.2	0.075	0.3

the flood events were utilized to validate the hydraulic model (Bhattarai et al., 2022; Mokhtar et al., 2018).

For a comprehensive flood vulnerability assessment, we considered economic, social, and environmental consequences (Gain et al., 2015). We overlaid the obtained inundation map with LULC and population data to analyze the socio-economic effects comprehensively. To assess population vulnerability, we considered economic activities such as occupation, industry involvement, caste/ethnicity, educational status, and gender, using the latest Nepal Census 2021 data obtained from (<https://censusednepal.cbs.gov.np/>). Ward-level statistics were available for education and household sizes, while economic and caste/ethnicity data were available up to the municipality/rural municipality level. The general scenario of education and economy of the different levels were comparable, so we performed the analysis with the view that it is representative data for vulnerability assessment (Figure 2).

### 3. Results and Discussion

#### 3.1. Flood Probability Distribution

The hydrological calculations from the LP-III, LN, GEV-I, and WB methods demonstrate probable flooding scenarios. Flood frequencies obtained from these methods are presented in Table 2. It can be observed that the variation is high for the estimated floods for different return periods. The variation of the flood magnitude for 2, 5, 25, 50, 100, 200, and 500-year return periods varies from around 100 m<sup>3</sup>/s to 1100 m<sup>3</sup>/s (Table 2). LN and LP-III distributions have higher variations between the upper and lower limits. These variations can be related to using log-transformed data in the calculations. A slight change in the value from logarithmic calculation shows a wide variation in the flood magnitude. The simulation of floods in the ungauged river basin is challenging from a scientific point of view as it increases uncertainty due to the absence of records (Tegos et al., 2022). Since frequency-based flood relationships are just estimates from limited data, the values of the flood or return period calculated are uncertain. The cause for this uncertainty is the length of the data period (Beven and Hall, 2014). We Performed a scenario-based analysis to overcome the uncertainties for effective decisions. The uncertainties are elevated due to climate change, so it would be of higher risk when the deterministic result is used. In an ideal model world, the effects of climate change can be evaluated by the scenarios rather than the climate and impact models that can convert the

scenario to the impacts (Hattermann et al., 2018). Since the flood's magnitudes, extent, and depth are beyond our control, our primary goal should be flood risk management, which includes floodplain zoning, proper land use planning, and awareness generation (Verkade and Werner, 2011).

#### 3.2. Goodness of Fit Test

Based on the goodness of fit test using the Kolmogorov-Smirnov (KS) test, the KS statistics and p-values for GEV-I, LN, and LP-III performed very well compared to WB. The p-values are higher than 0.05, and KS statistics are relatively low (Table 3) for these three methods, indicating a reasonably good fit. The p-value is also high, suggesting that the data is consistent with the distributions. Based on the KS test statistics, three methods seem applicable to the flood frequency analysis. WB method is also considered for the scenario analysis to overview the possible scenarios.

#### 3.3. Flood Inundation Area

The flood inundation model ran under different return periods demonstrates the flooding extent in the RRC. The extent of the inundation obtained under the simulations helps quantify the flood impact and analyze the potential damage. Besides the fact that there is a considerable variation in the magnitude of the flood estimated from different distribution methods and scenarios (Table 2), the variation of the flood inundation area is less. The variation in the inundation area for a 2- to 500-year return period flood ranges from 5.18 km<sup>2</sup> to 7.86 km<sup>2</sup>. The variation in the flood magnitude is more than tenfold; however, the variation in the inundation area is around 3 km<sup>2</sup> (Figure 3 and Figure 4). This scenario can be related to the topography of the catchment. Hills surround most areas of the Roshi River with very few plain areas, so the magnitude of the flood increases the flow depth. In contrast, the inundation area increases in relatively less area. However, if we look at the plain areas, such as the area near the Araniko highway, specifically the western part of the Banepa Municipality, and the area closer to the Panauti, the inundation area is high (see the zoomed-in area of Figure 3).

We chose the major part of the Roshi River and the Punyamata River near the Araniko highway instead of following the origin of the Roshi River because the western part of the Banepa Municipality is vulnerable to flood. This area is relatively plain, just at the bottom of the hills, with constricted drainage, facilitating the river's swelling almost yearly. Similarly, the section of the river near the

TABLE 2. Flood Discharge ( $m^3/s$ ) obtained from different methods of flood frequency analysis.

Return Period (Years)	GEV-I			LN			LP-III			WB		
	ML	UL	LL	ML	UL	LL	ML	UL	LL	ML	UL	LL
2	340	381	297	338	379	301	332	372	297	312	353	272
5	482	554	392	464	561	383	460	556	381	455	527	383
25	694	829	519	654	875	489	673	909	499	706	805	607
50	781	944	571	733	1015	529	770	1083	547	814	929	699
100	869	1058	623	812	1162	568	871	1273	596	922	1049	796
200	955	1172	676	893	1314	606	978	1482	646	1031	1166	896
500	1070	1323	747	1000	1526	656	1130	1790	713	1173	1336	1011

ML = Mostlikely, UL = Upper Limit and LL = Lower Limit

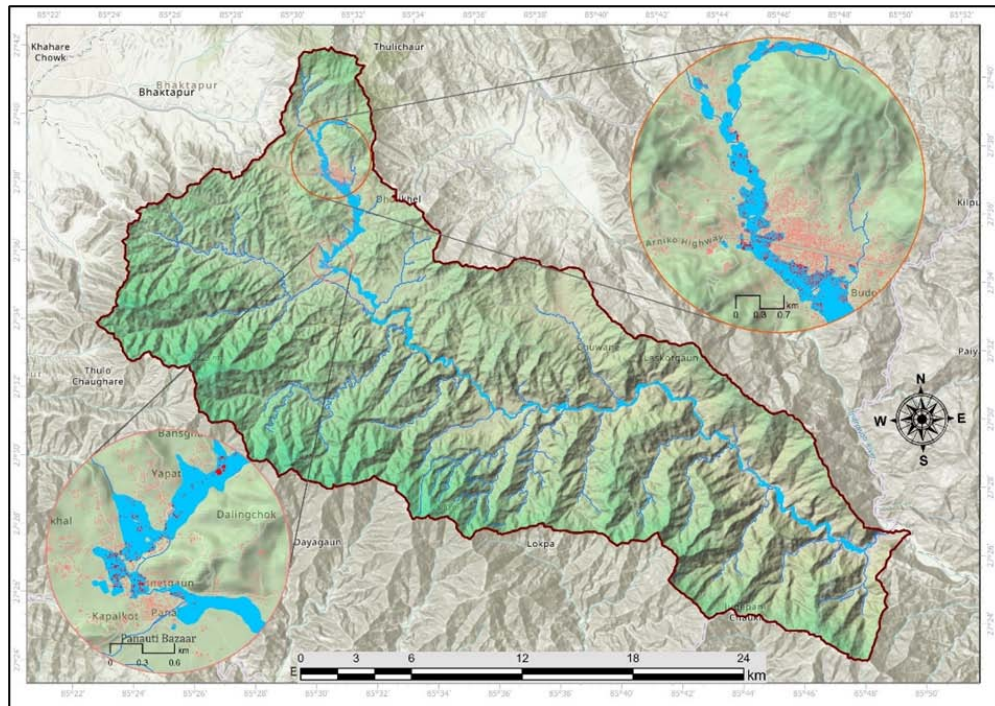


FIG. 3. Flood inundation map for different return periods (2, 5, 10, 25, 50, 100, 200, and 500) A) Flooded area near the Banepa Municipality near the Araniko Highway. B) Flooded area near the Panauti Area.

TABLE 3. Goodness of Fit test using the KS test.

	GEV-I	LN	LP-III	WB
KS statistic	0.107	0.101	0.091	0.777
p-value	0.691	0.763	0.852	0.000

Panauti Municipality is one of the important cultural cities of the country. This area is also prone to flooding periods (2, 5, 10, 25, 50, 100, 200, and 500) A) Flooded area near the Banepa Municipality near the Araniko Highway. B) Flooded area near the Panauti Area.

The Panauti area is a densely built-up area with a flat area made from a floodplain surrounded by hills. This area is affected by flood due to restrained drainage within a small flat area. Some photographs of the flooding in the Banepa and Panauti areas shown in Figure 5 clearly describe the flooding that occurs almost yearly.

### 3.4. Validation of the Flood Inundation Areas Using Field Observation

We used field observations and local people’s opinions to validate flood inundation data. All ground truth points matched the flood layers generated by hydrodynamic modeling. Among these points, 12 were within the 2-year flood,

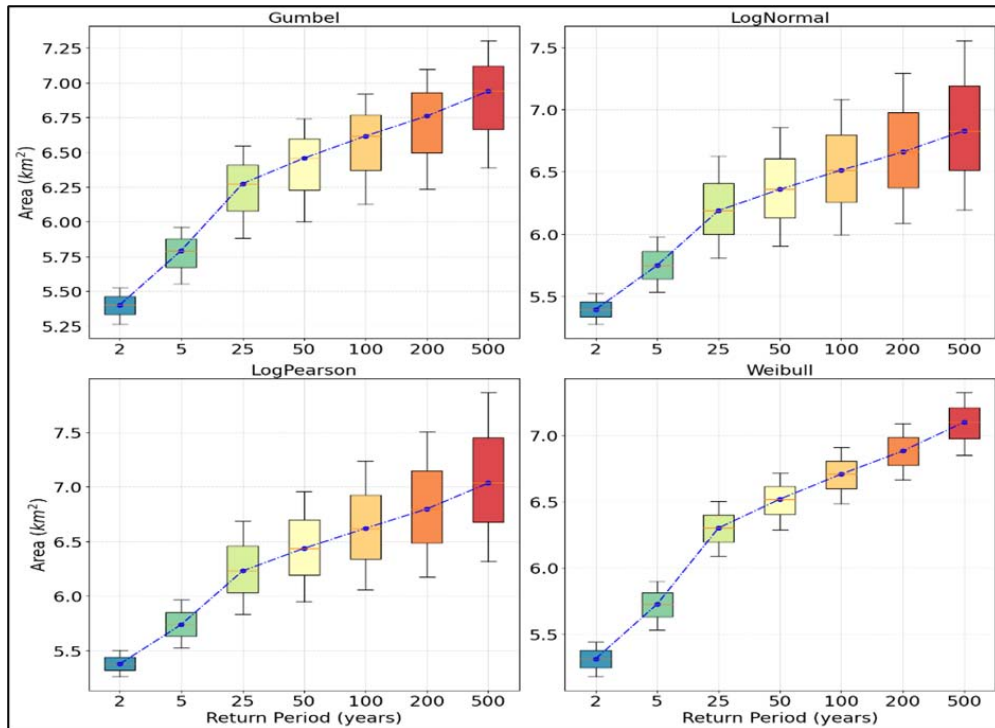


FIG. 4. Scenarios of flood inundation areas based on different distributions and return periods.



FIG. 5. Floods in Roshi, a b Punyamata River near Banepa (Sources a. <https://nepalnews.com/> b. [onlinekhbar.com](https://onlinekhbar.com/)), c. Namobuddha Village - rescue by Nepal Army (Source: <https://www.newsofnepal.com/>) d. Panauti Area near Indreshwor Temple Source: <https://www.recentnaturaldisasters.com/>

while 13 were within the 5, 10, and 25-year floods. For return periods of 50 to 500 years, 14 points were within each flood. It should be noted that there are overlapping points between different return period flood inundations.

To exemplify, the 2-year return period flood inundation lies within all the higher return period floods, implying the ground truth points. In summary, most points were in lower return period floods, while fewer were in higher

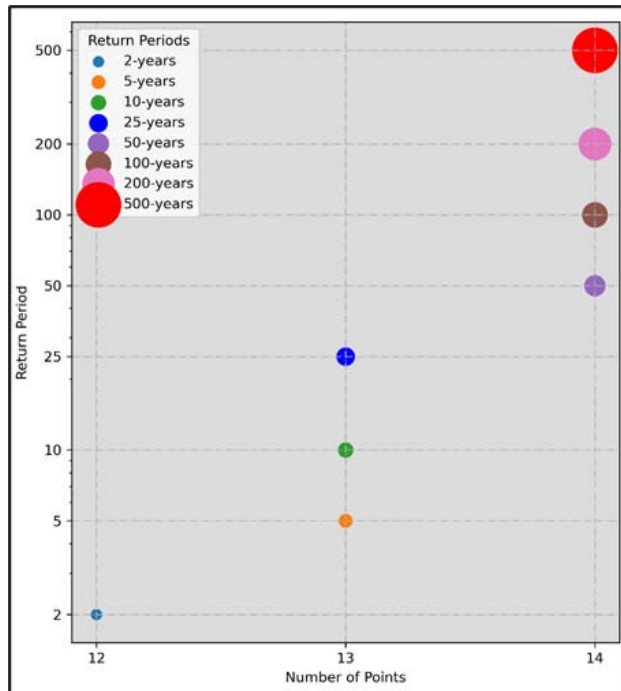


FIG. 6. Field validation data location according to the return period of flood.

return periods, confirming the model’s accuracy and enabling further analysis (Figure 6).

### 3.5. Vulnerability Assessment

The obtained results of the flood inundation area were exported for the flood hazard map with a population map and infrastructure files prepared with OSM. Based on four distributions and three scenarios of an upper limit, estimated flood, and lower limits from a 95% confidence interval and seven return periods, 84 flooding scenarios. The generated flood inundation area assessed the vulnerabilities to buildings, populations, and LULC classes. The analysis was performed using intersection and cross-tabulation tools.

#### 3.5.1. Inundation Scenario for LULC Classes

Based on these analyses, the LULC class that would be affected by flood is the cropland. The area that is probable to flood ranges from 385 to 573 ha. The variation of the predicted flooding to the cropland area according to the distributions is considerably low. According to the calculations, the most likely scenario is without the confidence limit. The area likely to flood ranges from 394 to 400 ha for a 2-year return period flood, whereas it ranges from 500 to 519 ha. for a 500-year return period flood. A similar scenario is observed for other LULC classes. The built-up area ranges from 44 to 82.5 ha, and the most likely area to

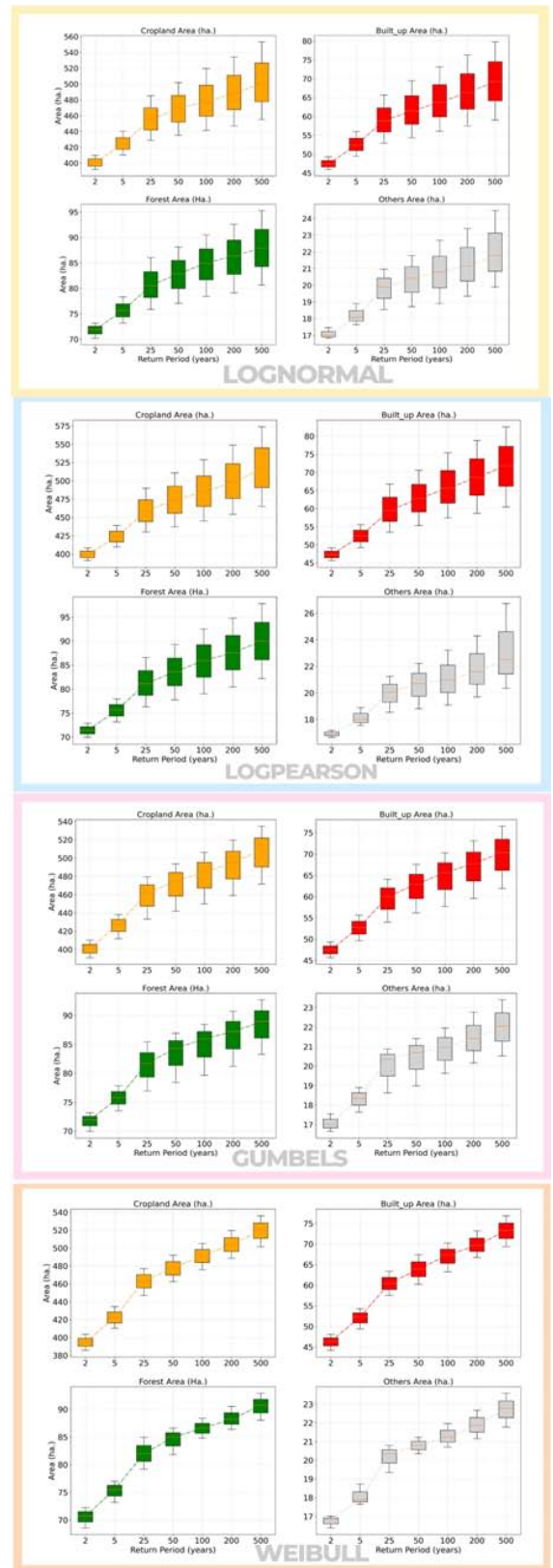


FIG. 7. Flood inundation area of different LULC classes.

be flooded in the built-up area ranges from 46 to 47 ha for a 2-year return period, whereas 69 to 73 ha for a 500-year return period flood. The forest area ranges from 68 to 97 ha, with the most likely range of 71 to 72 ha for a 2-year return period and 88 to 91 ha. for a 500-year return period. Another LULC class we considered for analysis was the other area, including the grassland, river bed, and other wood classes. The area ranges from 16 to 27 ha, with the most likely area for a 2-year return period flood as 18 ha and 22 to 23 ha for a 500-year return period (Figure 7).

### 3.5.2. Probable Effects on the Population and Buildings

The overlay of the flooding scenarios and population distribution layer showed the possible effect on the population of the RRC. The population variation affected by flood seems less for the return periods of 25 to 100-year return period floods than other return periods for all distributions. The probable number of people affected by flood ranges from 4091 to 6908. The most likely numbers of people that might be affected by the flood for a 2-year return period flood are 4200 to 4264 and 5768 to 6025. The estimates by WB distribution are comparatively lower for 2 and 5-year return periods, whereas it has the highest numbers for all other return periods. The ranges between upper and lower limits are similar for all the distributions (Figure 8).

The overlaid flood inundation scenario and the buildings shapefile showed the number of probable buildings to flood. The buildings layer contains almost all kinds of facilities, including residential buildings, office buildings, hospitals, community buildings, temples, and other monuments. The probable number of buildings that will be affected by flood varies from 1192 to 2570. Most likely, the estimated buildings that would be affected by flood range from 1257 to 1300 for the return periods of 2-year whereas the estimate for 500 years return period would be 1989 to 2154 (Figure 9). It can be observed that the variation between the upper limit and lower limits is relatively less for the WB distribution, which contrasts with the GEV-I, LN, and LP-III distributions. Careful consideration must be done while choosing an appropriate value to limit the effects due to the uncertainties related to data and methods. To minimize the impacts on the life and properties of the people vulnerable to the flood, we suggest using upper limits; however, the field condition and economic analysis must be done before the decision-making.

### 3.5.3. Status of Vulnerable Communities According to Economic Activities, Education, and Ethnicity

According to Nepal Census Report 2021, the economically active population aged ten years and above in Kavrepalanchok and Sindhuli District comprises 73.4% and 79.5%, respectively. Among them, most work in agriculture (65% in Kavrepalanchok and 77% in Sindhuli). Based on this census for each local government level,

i.e., municipality and rural municipality level, it can be noted that the percentage of economically active population varies from 66.2% in Banepa Municipality to 81.3% in Roshi Rural Municipality. Majority of this active population works in agriculture sector ranging from 35.8% in Banepa Municipality to 86.2% in Roshi Rural Municipality. The lower range of people working in the agriculture sector in Banepa is because a densely populated area in this municipality lives around the Araniko Highway, with more people engaged in business sectors such as wholesale, retail trade, manufacturing, and construction business. The area is also flood-prone, as shown in Figures 3 and 5. Likewise, in the case of municipalities with more people relying upon the agriculture field, floods can cause adverse effects on the economy as well as the daily life of the people. Most cultivated areas lie closer to the river due to water availability and fertile soil. Besides this, urban sprawl is also developed near rivers. This urban development can be attributed to major roads and highways nearby rivers. For example, the BP highway and Banepa-Panauti-Khopasi road are built close to the Roshi River, and major settlements and markets are closer to the roads. Due to this development, people with all kinds of economic activities are vulnerable to flooding. The literacy rates of Nepal, Bagmati Province, Kavrepalanchok, and Sindhuli, according to 2021, are 76.2%, 82.1%, 75.7%, and 72.6%, respectively. The male-to-female difference in literacy rates is of difference 12% to 16%. A similar trend can be seen in the literacy rate for all the wards connected to the flood-prone zones of the Roshi River. For example, the highest Literacy rate is in ward no. 7 of Banepa is near a high flood-prone area near Araniko Highway, and the lowest literacy rate is 55.67% in ward 9 of Temal Rural Municipality. In these wards, the differences between male and female literacy rates are comparable to National, Provincial, and district-level male-to-female literacy rate differences. The lowest difference is 7.2% in ward 9% of Temal Rural Municipality and the highest in ward 4 of the same Rural Municipality (Figure 10-h). The lower literacy rate and difference in male to female go in line with the ethnic distribution of the population. Most of the population in Kavrepalanchok district is Tamang, with 33.8%, followed by Brahman-hill-20.1%, Kshetri-13.6%, and Newa (Newar)-13.4%. The municipality-wise distribution shows the highest percentage is of Tamang in all municipalities in Kavrepalanchok except Banepa, with 28.2% Newa and 25.7% Brahman-hill in Panauti (Figure 10 e and f).

The comparison between ethnicity and literacy rate makes it more apparent that the literacy rate is lower in the areas where most of the population is Tamang (Figure 10 e, f, and g), with only the exception of Dhulikhel Municipality. In Dhulikhel Municipality, the percentages of Tamang, Brahman-hill, and Newa are similar at 25.6%, 24%, and 18.2% respectively. Based on ethnicity, Brahman and Kshetris, known to be the higher caste, are better

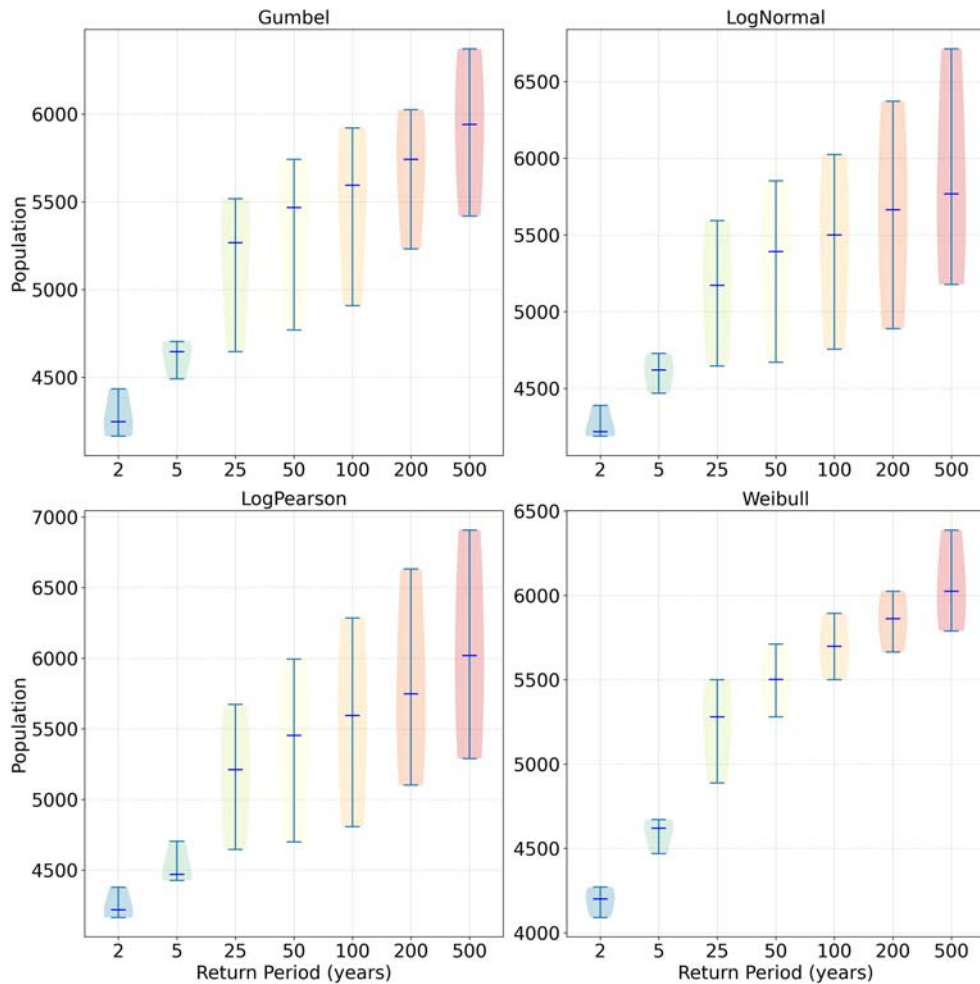


FIG. 8. Probable effects on the population due to flood.

in economic activities and educational status in the case of Nepal. The Janajatis and so-called lower castes have low income and literacy rates (Hatlebakk, 2017; Devkota and Bagale, 2015). Among Janajatis, Newa has a relatively lower poverty rate (Subba et al., 2014). It is evident from past experiences that natural hazards become a disaster when they hit vulnerable people. Vulnerability is the human dimension described by their physical condition and economy, or, in other words, it is a situation that defines the capacity of the people to resist the hazard (Guragain and Doney, 2022). With this definition, it can be easily understood that natural hazards might hit communities with the same magnitude, but the scale of their effect differs from their capacity (Yoon, 2012). For example, a community or people with access to resources can regain their potential faster than those deprived. The demographic composition of the RRC concerning the administrative units can be summarized as the people who depend on agriculture

are highly impacted by flood because the most affected area seems to be the agricultural area (Figure 7). Likewise, based on the literacy rate, economic activities, and ethnicity, Tamangs, with the highest population, are more vulnerable than Brahman, Kshetris, and Newa communities. Based on the flood inundation area, it seems that the areas inside Banepa Municipality and Panauti Municipality are vulnerable to flooding; however, even though flooding occurs every year, these areas regain normalcy easily compared to the others. This fact can be linked to the education, economic status, and profession of those living there. These areas mainly involve wholesale and retail trade, vehicle-related work, and financial and insurance activities (Figure 10). These professionals are linked to financial transactions that are less affected by floods except for disruption of daily activities due to flooding in flooding periods. However, the floods directly affect areas where people's professions relate to agriculture or river materials,

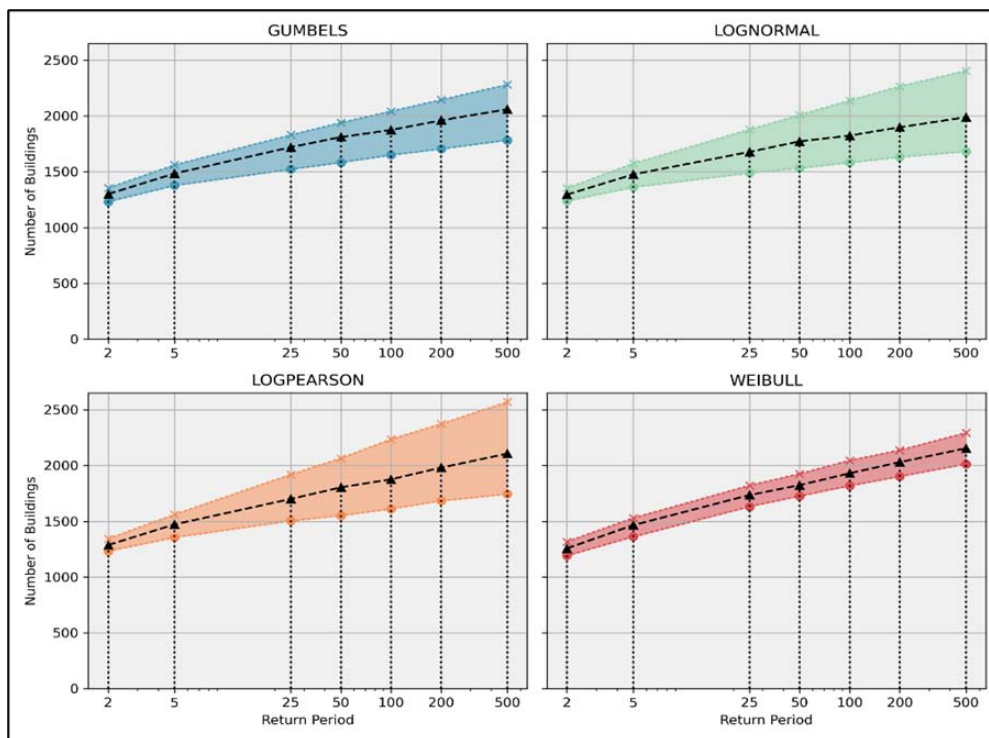


FIG. 9. No. of buildings that are probable to be inundated due to different return period floods.

such as sand mining and stone quarries. When people rely on agriculture, flooding the cultivated areas destroys the crops and agricultural products that make their lives miserable. In developing countries like Nepal, women are extensively engaged in agricultural work while fulfilling their reproductive responsibilities (Sugden and De Silva, 2014). Gender-based social norms significantly influence disaster responses. Research indicates that women are particularly vulnerable to disasters due to preexisting disadvantages in their social, economic, political, legal, and cultural status and limited opportunities (Ajibade et al., 2013; Yoon, 2012). This vulnerability is especially pronounced in developing nations, where many women and girls experience restricted access to crucial resources and decision-making processes, including information, finance, personal health, education, and rights. Insufficient training and education exacerbate the situation, leading many women into low-wage informal work, resulting in lower incomes. They may encounter difficulties diversifying their livelihoods or building resilience against flood-related challenges (Guragain and Doney, 2022). The situation in the RRC exemplifies notable disparities in women's involvement in economic activities and education. Overall, developing countries like Nepal exhibit higher vulnerability of women to disasters. Women's education deprivation affects their access to resources and economic activities, rendering them more susceptible to disasters such as floods. Similarly,

the imbalance in their roles within families makes women more reliant on agricultural activities, with the earnings from these activities controlled by men. Therefore, the vulnerability of women to disasters, particularly floods, is a complex issue followed by various socio-economic factors.

#### 4. Conclusion

Nepal is a Himalayan country with a significant variation in its topographical features over a relatively short latitudinal distance (i.e., North-South), which has led to the formation of steep slopes in numerous river catchments. In Nepal's case, the disaster's vulnerability is linked to extreme climatological events and exposure to them. The increased exposure can be related to the changed demography and the people's economy (Delalay et al., 2018). The poor people are the ones who are highly vulnerable due to exposure to flood hazards. For proper disaster management, education, skill development, adaptation, and resilience building are the major activities that governments of all levels must focus on, which need targeted focus group programs based on economic, educational, and vulnerability status. In the RRC, the anthropogenic activities without proper planning and policies, such as the development of Roads, sand mining, crusher industries, and constructions near the Roshi River, and the sediments originating from these activities, have escalated the flood risk, which

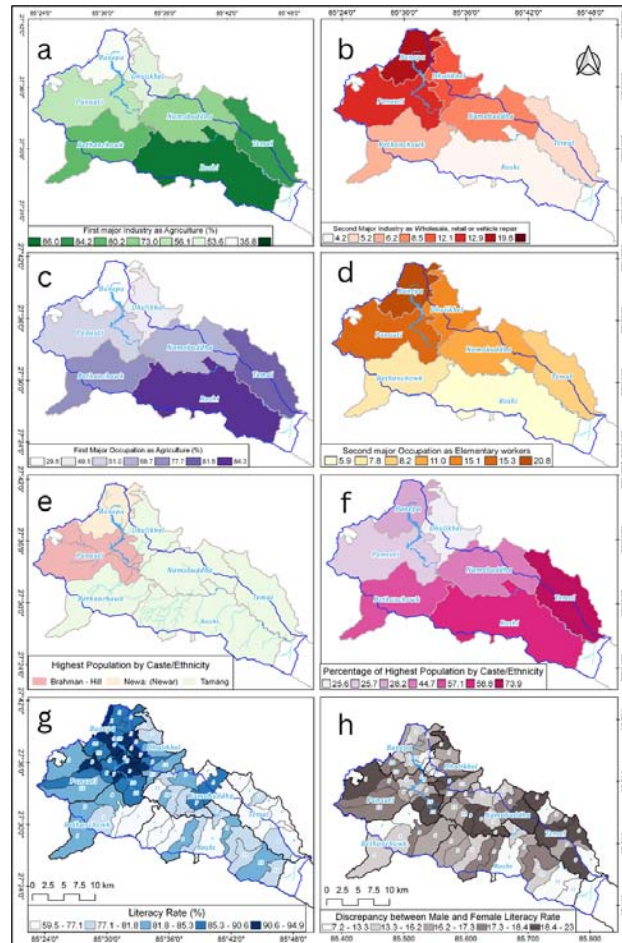


FIG. 10. Population composition in RRC according to Industry, Occupation, Caste/Ethnicity, and Educational status a) First major industry as agriculture b) Second Major industry as wholesale, retail or vehicle repair c) First major occupation as Agriculture d) Second major occupation as elementary workers e) Highest Population by caste/ethnicity f) Percentage of the highest population by caste/ethnicity g) Literacy rate (ward wise) h) Discrepancy in male and female literacy rate (Ward wise).

in turn increased the vulnerability by many folds. Besides this, more than two dozen crusher industries threatened the spring water sources crucial for drinking water supplies. While accounting for disaster management, the possible impact of changing climate is also crucial. For example, in the case of the RRC, agriculture is the main sector affected by floods. Most underprivileged communities depend on agriculture and live in flood-prone areas. Not only in the RRC, the general scenario of Nepal shows that the disruption in daily activities and dependency on the men who are also hit by disasters make women's conditions miserable. In this regard, more concern and awareness must be generated among women in economically and socially backward communities since they are more vulnerable to floods than others. Besides this, the local, provincial, and central governments must also have proactive plans in flood disaster management strategies, focusing on the socio-economically weak and marginalized community. In

the RRC, the Tamang community, being the most populous in number, is backward economically and in literacy rate, so special programs should be developed to uplift their educational and economic status, which will be a crucial step in flood disaster management. Likewise, the people involved in agricultural activities are more vulnerable, so the focus should be on proper floodplain management. Disaster prevention measures should be applied to communities dependent on agriculture. Since the Roshi River lacks a gauging system and the data obtained through interviews with locals may have some degree of uncertainty, our study did not have a comprehensive validation of the flood. However, the availability of ample satellite imagery and prominent high flood markings observed in the region contribute to identifying the flood extent. In this regard, the result from this study would be helpful for policymakers, planners, and decision-makers from all levels of state for the future since the RRC includes important

historical cities, such as Banepa, Dhulikhel, and Panauti, strategically important roads such as the Asian Highway (AH42) the Araniko Highway and BP highway that connects to the major eastern part of the country to the economically and strategically important Kathmandu Valley, i.e., the Capital city of Nepal. The effect of flooding this area not only disrupts the activities of the people there and the most economically active areas, such as major cities around the capital city, Kathmandu. In this regard, the hydrodynamic modeling presenting possible scenarios relating to socio-economic aspects would be beneficial in the decision-making process from local to central level government.

**Acknowledgments.** The authors thank Khwopa College of Engineering and Khwopa College for their support during the research. Similarly, we are thankful to the local respondents who supported us during the field visit for the ground-truthing of the flood areas.

## References

- Afzal, M. A., and Coauthors, 2022. Flood inundation modeling by integrating hec-ras and satellite imagery: a case study of the indus river basin. *Water*, 14 (19), 2984.
- Ajibade, I., G. McBean, and R. Bezner-Kerr, 2013. Urban flooding in lagos, nigeria: Patterns of vulnerability and resilience among women. *Global environmental change*, 23 (6), 1714–1725.
- Anzellini Vicente, F. P. C. S. F.-D. F. V. G. k. H. T. O. A. T. F. . Y. L., Cazabat Christelle, 2022. Disaster displacement in asia and the pacific: A business case for investment in prevention and solutions in asia and the pacific disaster displacement. <http://internal-displacement.org>.
- Aryal, D., L. Wang, T. R. Adhikari, J. Zhou, X. Li, M. Shrestha, Y. Wang, and D. Chen, 2020. A model-based flood hazard mapping on the southern slope of himalaya. *Water*, 12 (2), 540.
- Asquith, W. H., M. C. Roussel, and J. Vrabel, 2006. Statewide analysis of the drainage-area ratio method for 34 streamflow percentile ranges in texas. *US Geological Survey*.
- Beven, K. J., and J. Hall, 2014. Applied uncertainty analysis for flood risk management. *World Scientific*.
- Bhattacharai, R., U. Bhattacharai, V. P. Pandey, and P. K. Bhattacharai, 2022. An artificial neural network-hydrodynamic coupled modeling approach to assess the impacts of floods under changing climate in the east rapiti watershed, nepal. *Journal of Flood Risk Management*, 15 (4), e12 852.
- Bomers, A., R. M. Schielen, and S. J. Hulscher, 2019. Decreasing uncertainty in flood frequency analyses by including historic flood events in an efficient bootstrap approach. *Natural hazards and earth system sciences*, 19 (8), 1895–1908.
- Chow, V. T., 1959. Open-channel hydraulics mcgraw-hill book company, 1959. ISBN 07-010776-9.
- Chowdhury, J. U., and J. R. Stedinger, 1991. Confidence interval for design floods with estimated skew coefficient. *Journal of Hydraulic Engineering*, 117 (7), 811–831.
- Dangol, S., 2014. Use of geo-informatics in flood hazard mapping: A case of balkhu river. *Journal on Geoinformatics, Nepal*, 13, 52–57.
- Dangol, S., and A. Bormudoi, 2015. Flood hazard mapping and vulnerability analysis of bishnumati river, nepal. *Journal on Geoinformatics, Nepal*, 14, 20–24.
- Delalay, M., A. D. Ziegler, M. S. Shrestha, R. J. Wasson, K. Sudmeier-Rieux, B. G. McAdoo, and I. Kochhar, 2018. Towards improved flood disaster governance in nepal: a case study in sindhupalchok district. *International journal of disaster risk reduction*, 31, 354–366.
- Devkota, L. P., and D. R. Gyawali, 2015. Impacts of climate change on hydrological regime and water resources management of the koshi river basin, nepal. *Journal of Hydrology: Regional Studies*, 4, 502–515.
- Devkota, S. P., and S. Bagale, 2015. Social inequality in nepal and right of education. *Journal of Poverty, Investment and Development*, 8, 1–4.
- Dingle, E., M. Creed, H. Sinclair, D. Gautam, N. Gourmelen, A. Borthwick, and M. Attal, 2020. Dynamic flood topographies in the terai region of nepal. *Earth Surface Processes and Landforms*, 45 (13), 3092–3102.
- Emerson, D. G., A. V. Vecchia, and A. L. Dahl, 2005. Evaluation of drainage-area ratio method used to estimate streamflow for the red river of the north basin, north dakota and minnesota. *US Geological Survey*.
- Gain, A. K., V. Mojtabed, C. Biscaro, S. Balbi, and C. Giupponi, 2015. An integrated approach of flood risk assessment in the eastern part of dhaka city. *Natural Hazards*, 79, 1499–1530.
- Guragain, U. P., and P. Doneys, 2022. Social, economic, environmental, and physical vulnerability assessment: An index-based gender analysis of flood prone areas of koshi river basin in nepal. *Sustainability*, 14 (16), 10 423.
- Halbert, K., C. C. Nguyen, O. Payrastra, and E. Gaume, 2016. Reducing uncertainty in flood frequency analyses: A comparison of local and regional approaches involving information on extreme historical floods. *Journal of Hydrology*, 541, 90–98.
- Hatlebakk, M., 2017. Nepal: A political economy analysis. *Report*.
- Hattermann, F., and Coauthors, 2018. Sources of uncertainty in hydrological climate impact assessment: a cross-scale study. *Environmental Research Letters*, 13 (1), 015 006.
- Hosseiny, H., F. Nazari, V. Smith, and C. Nataraj, 2020. A framework for modeling flood depth using a hybrid of hydraulics and machine learning. *Scientific Reports*, 10 (1), 8222.
- Jha, A. K., and Coauthors, 2016. Impact of irrigation method on water use efficiency and productivity of fodder crops in nepal. *Climate*, 4 (1), 4.
- Lamichhane, S., and N. M. Shakya, 2019. Integrated assessment of climate change and land use change impacts on hydrology in the kathmandu valley watershed, central nepal. *Water*, 11 (10), 2059.
- Maposa, D., J. J. Cochran, and M. Lesaoana, 2014. Investigating the goodness-of-fit of ten candidate distributions and estimating high quantiles of extreme floods in the lower limpopo river basin, mozambique. *Journal of Statistics and Management Systems*, 17 (3), 265–283.

- McFeeters, S. K., 1996. The use of the normalized difference water index (ndwi) in the delineation of open water features. *International journal of remote sensing*, 17 (7), 1425–1432.
- Merz, B., and A. H. Thielen, 2005. Separating natural and epistemic uncertainty in flood frequency analysis. *Journal of Hydrology*, 309 (1-4), 114–132.
- Merz, B., and Coauthors, 2021. Causes, impacts and patterns of disastrous river floods. *Nature Reviews Earth & Environment*, 2 (9), 592–609.
- Mokhtar, E. S., B. Pradhan, A. H. Ghazali, and H. Z. M. Shafri, 2018. Assessing flood inundation mapping through estimated discharge using gis and hec-ras model. *Arabian Journal of Geosciences*, 11, 1–20.
- Namara, W. G., T. A. Damisse, and F. G. Tufa, 2022. Application of hec-ras and hec-georas model for flood inundation mapping, the case of awash bello flood plain, upper awash river basin, oromiya regional state, ethiopia. *Modeling Earth Systems and Environment*, 8 (2), 1449–1460.
- Pathak, S., H. K. Panta, T. Bhandari, and K. P. Paudel, 2020. Flood vulnerability and its influencing factors. *Natural Hazards*, 104, 2175–2196.
- Pinos, J., and L. Timbe, 2019. Performance assessment of two-dimensional hydraulic models for generation of flood inundation maps in mountain river basins. *Water science and engineering*, 12 (1), 11–18.
- Poudel, L., B. Thapa, B. P. Shrestha, and N. K. Shrestha, 2012. Impact of sand on hydraulic turbine material: A case study of roshi khola, nepal. *Hydro Nepal: Journal of Water, Energy & Environment*, (10).
- Rahman, A. S., A. Rahman, M. A. Zaman, K. Haddad, A. Ahsan, and M. Imteaz, 2013. A study on selection of probability distributions for at-site flood frequency analysis in australia. *Natural hazards*, 69, 1803–1813.
- Razavi, T., and P. Coulibaly, 2013. Streamflow prediction in ungauged basins: review of regionalization methods. *Journal of hydrologic engineering*, 18 (8), 958–975.
- Sarchani, S., K. Seiradakis, P. Coulibaly, and I. Tsanis, 2020. Flood inundation mapping in an ungauged basin. *Water*, 12 (6), 1532.
- Sharma, A. P., X. Fu, and G. R. Kattel, 2023. Is there a progressive flood risk management in nepal? a synthesis based on the perspective of a half-century (1971–2020) flood outlook. *Natural Hazards*, 1–21.
- Sharma, T. P. P., J. Zhang, U. A. Koju, S. Zhang, Y. Bai, and M. K. Suwal, 2019. Review of flood disaster studies in nepal: A remote sensing perspective. *International journal of disaster risk reduction*, 34, 18–27.
- Shreevastav, B. B., K. R. Tiwari, R. A. Mandal, and A. Nepal, 2021. Assessing flood vulnerability on livelihood of the local community: A case from southern bagmati corridor of nepal. *Progress in Disaster Science*, 12, 100 199.
- Singh, R. M., 2018. Fishing for a cause in roshi: How we saw a river depleted, degraded and violated. *Onlinekhabar*. <https://english.onlinekhabar.com/fishing-for-a-cause-in-roshi-how-we-saw-a-river-depleted-degraded-and-violated.html>.
- Sofia, G., and E. I. Nikolopoulos, 2020. Floods and rivers: A circular causality perspective. *Scientific reports*, 10 (1), 5175.
- Subba, C., B. Pyakuryal, T. Bastola, M. Subba, N. Raut, and B. Karki, 2014. A study on socio-economic status of indigenous peoples in nepal. *Lawyers' Association for Human Rights of Nepalese Indigenous Peoples (LAHURNIP) and The International Work Group for Indigenous Affairs (IWGIA)*.
- Sugden, F., and S. De Silva, 2014. A framework to understand gender and structural vulnerability to climate change in the ganges river basin: lessons from bangladesh, india and nepal.
- Talchabhadel, R., R. Karki, B. R. Thapa, M. Maharjan, and B. Parajuli, 2018. Spatio-temporal variability of extreme precipitation in nepal. *International Journal of Climatology*, 38 (11), 4296–4313.
- Talchabhadel, R., and Coauthors, 2021. Insights on the impacts of hydroclimatic extremes and anthropogenic activities on sediment yield of a river basin. *Earth*, 2 (1), 32–50.
- Tamiru, H., and M. O. Dinka, 2021. Application of ann and hec-ras model for flood inundation mapping in lower baro akobo river basin, ethiopia. *Journal of Hydrology: Regional Studies*, 36, 100 855.
- Tegos, A., A. Ziogas, V. Bellos, and A. Tzimas, 2022. Forensic hydrology: A complete reconstruction of an extreme flood event in data-scarce area. *Hydrology*, 9 (5), 93.
- Tellman, B., J. A. Sullivan, C. Kuhn, A. J. Kettner, C. S. Doyle, G. R. Brakenridge, T. A. Erickson, and D. A. Slayback, 2021. Satellite imaging reveals increased proportion of population exposed to floods. *Nature*, 596 (7870), 80–86.
- Thapa, S., A. Shrestha, S. Lamichhane, R. Adhikari, and D. Gautam, 2020. Catchment-scale flood hazard mapping and flood vulnerability analysis of residential buildings: The case of khando river in eastern nepal. *Journal of Hydrology: Regional Studies*, 30, 100 704.
- UNDRR, 2019. Disaster risk reduction in nepal: Status report 2019. *Disaster Aster Risk Reduction of Nepal*, 1–28. [https://www.preventionweb.net/files/68257\\_682306nepaldrmrstatusreport](https://www.preventionweb.net/files/68257_682306nepaldrmrstatusreport).
- Verkade, J., and M. Werner, 2011. Estimating the benefits of single value and probability forecasting for flood warning. *Hydrology and Earth System Sciences*, 15 (12), 3751–3765.
- Yin, J., P. Gentile, S. Zhou, S. C. Sullivan, R. Wang, Y. Zhang, and S. Guo, 2018. Large increase in global storm runoff extremes driven by climate and anthropogenic changes. *Nature communications*, 9 (1), 4389.
- Yoon, D. K., 2012. Assessment of social vulnerability to natural disasters: a comparative study. *Natural hazards*, 63, 823–843.
- Yue, S., T. B. Ouarda, B. Bobée, P. Legendre, and P. Bruneau, 1999. The gumbel mixed model for flood frequency analysis. *Journal of hydrology*, 226 (1-2), 88–100.
- Zotou, I., V. Bellos, A. Gkouma, V. Karathanassi, and V. A. Tsihrintzis, 2020. Using sentinel-1 imagery to assess predictive performance of a hydraulic model. *Water Resources Management*, 34, 4415–4430.
- Zotou, I., K. Karamvavis, V. Karathanassi, and V. A. Tsihrintzis, 2022. Potential of two sar-based flood mapping approaches in supporting an integrated 1d/2d hec-ras model. *Water*, 14 (24), 4020.